Active Site Plasticity in D-Amino Acid Oxidase: A Crystallographic Analysis[†,‡]

Flavia Todone,[§] Maria Antonietta Vanoni,[∥] Andrea Mozzarelli,[⊥] Martino Bolognesi,[§,▽] Alessandro Coda,[§] Bruno Curti,[∥] and Andrea Mattevi*[,§]

Dipartimento di Genetica e Microbiologia, Università di Pavia, Via Abbiategrasso 207, 27100 Pavia, Italy, Dipartimento di Fisiologia e Biochimica Generali, Università di Milano, Via Celoria 26, 20133 Milano, Italy, Istituto di Scienze Biochimiche, Università di Parma, Viale delle Scienze, 43100 Parma, Italy, and Dipartimento di Fisica and Centro per le Biotecnologie Avanzate, Università di Genova, Largo R. Benzi 10, 16132 Genova, Italy

Received December 12, 1996; Revised Manuscript Received January 22, 1997[⊗]

ABSTRACT: D-Amino acid oxidase (DAAO) is the prototype of the flavin-containing oxidases. It catalyzes the oxidative deamination of various D-amino acids, ranging from D-Ala to D-Trp. We have carried out the X-ray analysis of reduced DAAO in complex with the reaction product imino tryptophan (iTrp) and of the covalent adduct generated by the photoinduced reaction of the flavin with 3-methyl-2-oxobutyric acid (kVal). These structures were solved by combination of 8-fold density averaging and least-squares refinement techniques. The FAD redox state of DAAO crystals was assessed by single-crystal polarized absorption microspectrophotometry. iTrp binds to the reduced enzyme with the N, Cα, C, and Cβ atoms positioned 3.8 Å from the *re* side of the flavin. The indole side chain points away from the cofactor and is bound in the active site through a rotation of Tyr224. This residue plays a crucial role in that it adapts its conformation to the size of the active site ligand, providing the enzyme with the plasticity required for binding a broad range of substrates. The iTrp binding mode is fully consistent with the proposal, inferred from the analysis of the native DAAO structure, that substrate oxidation occurs via direct hydride transfer from the Cα to the flavin N5 atom. In this regard, it is remarkable that, even in the presence of the bulky iTrp ligand, the active center is made solvent inaccessible by loop 216−228. This loop is thought to switch between the "closed" conformation observed in the crystal structures and an "open" state required for substrate binding and product release. Loop closure is likely to have a role in catalysis by increasing the hydrophobicity of the active site, thus making the hydride transfer reaction more effective. Binding of kVal leads to keto acid decarboxylation and formation of a covalent bond between the keto acid Cα and the flavin N5 atoms. Formation of this acyl adduct results in a nonplanar flavin, characterized by a 22° angle between the pyrimidine and benzene rings. Thus, in addition to an adaptable substrate binding site, DAAO has the ability to bind a highly distorted cofactor. This ability is relevant for the enzyme's function as a highly efficient oxidase.

Flavin-containing enzymes can be grouped into a small number of classes whose members share several catalytic and chemical properties. The oxidase class is characterized by the ability of the reduced flavin to react rapidly with oxygen, yielding hydrogen peroxide and the oxidized cofactor (Massey, 1995). Other features common to the oxidases are their reactivity toward sulfite and their ability to stabilize the anionic form of the reduced flavin (Ghisla & Massey, 1989). The prototype of the oxidase class of flavoproteins is D-amino acid oxidase (DAAO[1]) which, since its discovery by Krebs (1935), has been the subject of a number of biochemical, functional, and kinetic investigations [see Curti et al. (1992)]. The enzyme catalyzes the oxidative deamination of D-amino acids to the corresponding α-keto acids, according to the scheme

$$RCHNH_2COOH + \text{E-FAD} \rightarrow RC{=}NHCOOH + \text{E-FADH}_2 \quad (1)$$

$$\text{E-FADH}_2 + O_2 \rightarrow \text{E-FAD} + H_2O_2 \quad (2)$$

$$RC{=}NHCOOH + H_2O \rightarrow RCOCOOH + NH_3 \quad (3)$$

The reductive half-reaction (eq 1), in which the FAD cofactor becomes reduced, is followed by FAD reoxidation through molecular oxygen with formation of hydrogen peroxide (eq 2). The imino acid product hydrolyzes spontaneously to the corresponding keto acid, in a nonenzymatic process (eq 3).

[†] This research was supported by grants from Ministero per l'Università e la Ricerca Scientifica e Tecnologica (MURST 60% to B.C. and A.C.) and Consiglio Nazionale delle Ricerche (Contract 9502988CT14 to B.C. and Contract 9502989CT14 to A.M.). We thank the European Union for support of the work at EMBL Hamburg through the HCMP to Large Installations Project (Contract CHGE-CT93-0040).

[‡] Coordinates have been deposited in the Protein Data Bank and assigned the ID codes 1DDO and 1DAO.

* Corresponding author: Andrea Mattevi, Dipartimento di Genetica e Microbiologia, Università di Pavia, Via Abbiategrasso 207, 27100 Pavia, Italy. Telephone: -39-382-505560. Fax: -39-382-528496. E-mail: MATTEVI@IPVGEN.UNIPV.IT.

[§] Università di Pavia.

[∥] Università di Milano.

[⊥] Università di Parma.

[▽] Università di Genova.

[⊗] Abstract published in *Advance ACS Abstracts,* March 1, 1997.

[1] Abbreviations: DAAO, D-amino acid oxidase (EC 1.4.3.3); Bz, benzoate; iArg, imino arginine; iTrp, imino tryptophan; kVal, 3-methyl-2-oxobutyric acid; NCS, non crystallographic symmetry; rms, root-mean-square.

S0006-2960(96)03057-7 CCC: $14.00

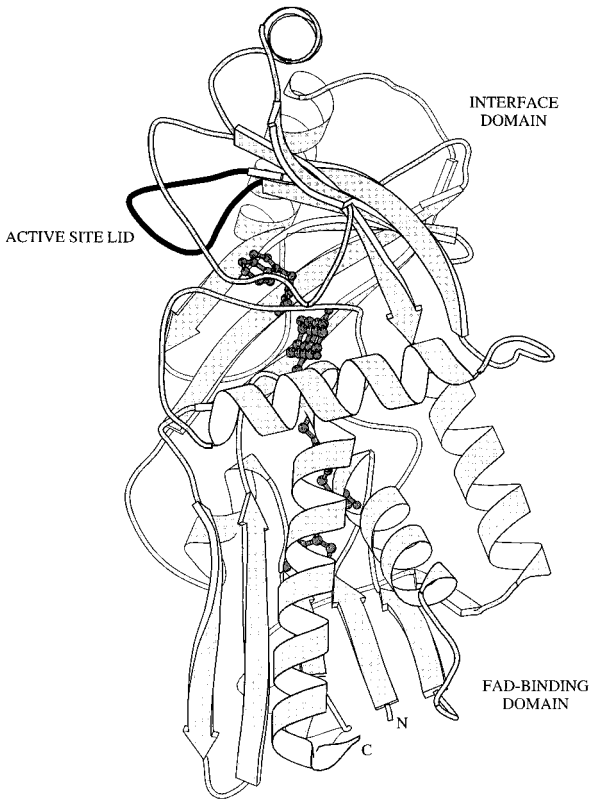

FIGURE 1: MOLSCRIPT (Kraulis, 1991) diagram of the reduced DAAO subunit in complex with iTrp. The letters N and C identify the N terminus and the C terminus of the protein, respectively. FAD and iTrp ball-and-stick drawings are shown in darker gray. The loop region comprising residues 216−228 (the active site lid) is shown in black.

The enzyme is strictly stereospecific and is able to oxidize a variety of D-amino acids, with a preference for those having small hydrophobic side chains (up to four C atoms), followed by those bearing polar, aromatic, and basic groups (Dixon & Kleppe, 1965). DAAO is completely inactive on acidic amino acids, for which a specific D-aspartate oxidase, sharing 50% identity with DAAO, is known (Negri et al., 1987).

The biological role of DAAO, a peroxisomal enzyme, is still uncertain. It has been suggested that the enzyme acts as a detoxifying agent, which removes D-amino acids accumulated during aging (D'Aniello et al., 1993). Indeed, D-amino acids have been detected in various human tissues such as teeth and blood (D'Aniello et al., 1993, and references therein). Moreover, it has been shown (Schell et al., 1995) that the human brain contains endogenous D-Ser, which is likely to function as a modulator of neurotransmission. On this basis, it has been speculated that DAAO may have a role in the metabolism of neurotransmitters, a hypothesis supported by the fact that the DAAO expression in the human brain is high (Fukui, 1996).

In spite of the number of biochemical, spectroscopic, and kinetic studies (Curti et al., 1992; Denu & Fitzpatrick, 1994), the mechanism of DAAO catalytic reaction has remained controversial. The so-called "carboanion" hypothesis (Walsh et al., 1973) predicts that substrate oxidation occurs via a carboanion intermediate, whose formation should be triggered by an active site base abstracting the substrate α-proton. Alternatively, it has been proposed that the amino acid substrate can be oxidized by direct transfer of a hydride to the flavin N5 position from either the substrate Cα (Hersh & Schuman Jorns, 1975) or N (Miura & Miyake, 1988) atoms. However, in the absence of the DAAO three-dimensional structure, neither of these proposals found definitive experimental support.

The crystal structure of DAAO from pig kidney, in complex with the competitive inhibitor benzoate (DAAO·Bz), has recently been solved in our groups (Mattevi et al., 1996) and by Mizutani et al. (1996). The enzyme is a dimer of 2 × 347 amino acids with one molecule of noncovalently bound FAD per subunit (Figure 1). Analysis of the structure revealed that the catalytic and substrate binding site is located in a hydrophobic cavity, made solvent inaccessible by a loop formed by residues 216−228 (Figure 1). This feature led to the proposal that this loop could function as an "active site lid", switching between the "closed" conformation observed in the DAAO·Bz complex and an "open" state, required to allow substrate binding and product release (Mattevi et al., 1996). The role played by the loop is further highlighted by the fact that the volume of the active site cavity (170 $Å^3$) matches the size of an amino acid having a four-carbon atom side chain. If this fact, on one hand, explained the enzyme preference for small hydrophobic substrates, on the other, it raised the question of how DAAO can bind and oxidize, though slowly, bulkier amino acids such as D-Trp, D-Phe, and D-Arg.

In this report, we describe the crystal structures of reduced DAAO in complex with the reaction product imino tryptophan (iTrp) and of the covalent addition product of DAAO with 3-methyl-2-oxobutyric acid (kVal). Comparison of these structures with the DAAO·Bz complex improves our understanding of substrate recognition and reactivity in this enzyme.

MATERIALS AND METHODS

Crystallization and Crystal Soaking. Native DAAO in complex with the inhibitor benzoate was crystallized by the hanging drop method at pH 8.3 using 0.6 M ammonium succinate as precipitant (Mattevi et al., 1996). The crystals belong to space group $C222_1$ with cell dimensions $a = 328$ Å, $b = 138$ Å, and $c = 201$ Å and eight enzyme subunits in the asymmetric unit (317 000 Da). For soaking, crystals were transferred to an air-saturated solution containing 20 mM ligand, 1.3 M ammonium succinate, and 100 mM Tris/HCl at pH 8.3. The soaking time was 48 h in each case.

Microspectrophotometric Studies. Single-crystal polarized absorption spectra (Mozzarelli & Rossi, 1996) were obtained using a Zeiss MPM800 microspectrophotometer, with crystals in their soaking solution placed in a flow cell with quartz windows. The orthorhombic DAAO crystals usually grow with the *c* axis along their shortest edge. On this basis, spectra could be recorded with the electric vector of linearly polarized light parallel to both *a* and *b* axes. Care was taken to carry out the microspectrophotometry experiments under conditions identical to those employed for the preparation of the crystals used in data collection.

X-ray Data Collection and Processing. Upon soaking, the DAAO crystals became very radiation sensitive, making the usage of the cryocrystallographic technique mandatory. Crystals were washed for a few seconds in a solution containing 25% (w/v) glycerol, 20 mM ligand, 1.3 M ammonium succinate, and 100 mM Tris/HCl at pH 8.3 and

Table 1: X-ray Diffraction Data

	$DAAO_{red}$·iTrp	D-Arg soaking	$DAAO_{red}$·kVal
unit cell axes (Å)	325.2, 137.1, 196.8	327.1, 137.6, 198.3	326.4, 136.9, 196.5
resolution limit (Å)	3.1	3.2	3.2
measured reflections	514 100	568 661	433 795
unique reflections	77 977	70 704	72 287
R_{merge}[a] (%)[b]	9.3 (23.6)	8.2 (27.9)	11.2 (35.2)
completeness (%)[b]	98.9 (98.7)	96.9 (96.3)	99.8 (99.1)

[a] $R_{merge} = \Sigma|I_j - \langle I_j\rangle|/\Sigma\langle I_j\rangle$, where I_j is the intensity of an observation of reflection j and $\langle I_j\rangle$ is the average intensity for reflection j. [b] In brackets, the value for the highest resolution shell is given.

then mounted on a thread loop to be flash frozen at 100 K under a stream of nitrogen. Freezing led to 1−2% shrinkage of the unit cell parameters (Table 1).

Diffraction data were collected on the X-ray diffraction beam line at the ELETTRA synchrotron source (Trieste, Italy), for the crystal soaked in D-Trp, and on the beam lines BW7 and X11 at DESY (Hamburg, Germany), for the crystals soaked in kVal and D-Arg, respectively. In all experiments, a 180 mm diameter Hendrix-Lentfer image plate was used with monochromatized radiation ($\lambda = 0.9$ Å). Data were integrated, scaled, and merged with the programs DENZO and SCALEPACK (Otwinoski, 1993). The data collection statistics are reported in Table 1.

Structure Solution and Refinement. The asymmetric unit of the crystals contains eight DAAO monomers that are related by local symmetry. Analysis of the three-dimensional structures was initiated by rigid-body refinement (eight independent subunits) of the native DAAO model (Mattevi et al., 1996) against the respective diffraction data using the program TNT (Tronrud et al., 1987). The resulting models were used for the calculation of the local symmetry operators. Phase refinement was performed by cyclic averaging using the program DM of the CCP4 package (Collaborative Computational Project Number 4, 1994). In order to minimize model bias, model building of ligands and active site residues was carried out employing "averaged-omit" electron density maps. These were generated by averaging the electron density maps calculated by omitting from phase calculation all residues within 5 Å of the flavin.

Model building was carried out with the program O (Jones et al., 1991), whereas the crystallographic refinement was performed with the program TNT (Tronrud et al., 1987). No σ cutoff was applied, and all measured reflections in the 20−3.1 Å range were used for refinement. Strict noncrystallographic symmetry (NCS) constraints (eight identical subunits) were applied so that the number of observations per the number of parameters was at least 6 in all refined structures. The only residues excluded from NCS constraints belonged to the "active site loop" of 216−228 (Figure 1), which is thought to change its conformation during the catalytic reaction (see below). The progress of the crystallographic analysis was monitored by the "free" R_{factor} (Brünger, 1992), calculated with 1000 reflections omitted from refinement. In the case of the complex with iTrp, a total of 107 ordered water molecules were located at positions with a density of $>1\sigma$ in the $2F_o - F_c$ map and $>4\sigma$ in the $F_o - F_c$ map. In the case of the complex with kVal, a strong electron density peak in the active center of all eight crystallographically independent subunits has been interpreted as an ordered water molecule, which, therefore, has been added to the refined model.

RESULTS

Crystal Preparation and Microspectrophotometric Analysis. Complexes of DAAO with the reaction products were prepared by soaking the native benzoate crystals in either 20 mM D-Trp or D-Arg. Upon soaking, the color of the crystals changed from bright yellow (typical of the oxidized protein) to a pale color, indicating that the enzyme was presumably in the reduced state. This was very unexpected, since the soaking experiments were carried out in an air-saturated environment and, by analogy with the enzyme reactivity in solution, flavin oxidation by oxygen was expected to occur.

We analyzed the outcome of the soaking experiments by single-crystal microspectrophotometry (Mozzarelli & Rossi, 1996). Polarized absorption spectra of a native DAAO crystal were very similar to that of the protein in solution and fully consistent with the presence of the complex between the oxidized enzyme and benzoate (Figure 2a). Moreover, spectra of DAAO crystals soaked in D-Arg and D-Trp (panels b and c of Figure 2) clearly showed that soaking in both amino acids led to enzyme reduction. Only in the case of D-Arg did the absorbance at 370 nm indicate that some of the crystalline enzyme molecules might be present as the red semiquinone (Curti et al., 1992). Absorption spectra were measured also from crystals soaked for 2 days in 20 mM substrate and then transferred again in the standard storage solution (1.3 M ammonium succinate, 100 mM Tris/HCl at pH 8.3, and no substrate). Upon such a "back-soaking" procedure, the crystals acquired within a few seconds the standard yellow color, with a spectrum indicative of a fully oxidized enzyme (Figure 2b). Moreover, the shoulder at 490 nm, typical of the DAAO·Bz complex (Figure 2a), was absent, indicating that benzoate had been displaced from the active site. These data revealed that reoxidation is possible even in the crystalline state and that it is the presence of an excess of substrate which protects the crystals from reoxidation.

α-Keto acids bearing small hydrophobic side chains are competitive inhibitors of DAAO (Dixon & Kleppe, 1965). Moreover, in the presence of light, these compounds decarboxylate and react with the flavin, producing a covalent adduct between the keto acid Cα and the flavin N5 atoms (Ghisla et al., 1979; DeKok et al., 1974). We studied the structure of such a covalent adduct by soaking the crystals in 3-methyl-2-oxobutyric acid, the keto acid structurally related to valine (kVal). The experiment was carried out in the presence of light. The microspectrophotometric analysis confirmed the occurrence of the photoinduced reaction, leading to the acyl adduct formation (Figure 2d).

X-ray Analysis and Overall Structure. Diffraction data were collected from crystals soaked in D-Trp ($DAAO_{red}$·

iTrp), D-Arg, and kVal ($DAAO_{red}$·kVal). Due to the limited diffraction power, data could be collected only up to 3.1−3.2 Å resolution. However, the 8-fold noncrystallographic symmetry within the DAAO crystal asymmetric unit allowed substantial improvement of the maps. For all the experiments, the 8-fold averaged maps were of good quality, allowing detailed interpretation of the active site residues (Figure 3a). The refinement of the models (Table 2) was performed with strict NCS constraints (number of observations per number of parameters ratio of at least 6), except for the polypeptide segment of 216−228. These residues form the active site lid (Figure 1) and were excluded from the NCS constraints to check for the presence of different loop conformations in the crystallographically independent subunits. PROCHECK (Laskowski et al., 1993) analysis indicates that the final models have stereochemical parameters well within the standard values. Particularly, all the main chain torsion angles fall within the allowed regions of the Ramachandran plot. The refinement statistics are listed in Table 2.

In all complexes, soaking did not lead to any significant change in the overall structure (Figure 1). The root-mean-square (rms) deviation from the 339 Cα positions of the DAAO·Bz structure (Mattevi et al., 1996) is 0.35 Å for the $DAAO_{red}$·iTrp complex, 0.44 Å for the D-Arg soaked structure, and 0.28 Å for the $DAAO_{red}$·kVal adduct.

$DAAO_{red}$·iTrp Complex. Soaking in D-Trp led to full reduction of the DAAO crystals (Figure 2c). The averaged electron density map showed a strong peak close to the flavin ring. A iTrp molecule fits well in this peak, suggesting that upon D-Trp soaking a $DAAO_{red}$·iTrp complex is formed[2] (Figure 3a). iTrp binds with the plane formed by the N, Cα, C, and Cβ atoms approximately parallel to the *re* face of the flavin, 3.8 Å from the cofactor (Figure 3b). The iTrp carboxylate group makes a strong H bond with the OH of Tyr228 (2.6 Å) and a salt bridge with Arg283 (3.2 Å to Nϵ and 3.5 Å to Nη2), while the imino group weakly interacts with the carbonyl oxygen of Gly313 (3.4 Å). The indole side chain points away from FAD and stacks over the benzene ring of Tyr224, being surrounded by several hydrophobic side chains delimiting the active site (Ala49, Leu51, Ile215, Ile230, and Tyr228).

Loop 216−228 (Figures 1 and 3b) is of considerable interest because in the DAAO·Bz complex it forms a lid, making the active center solvent inaccessible. In the $DAAO_{red}$·iTrp complex, the loop is well-defined in six of the eight crystallographically independent subunits (Figure 3a), whereas in two monomers, the loop has continuous density only at a relatively low (0.6−0.7σ) contour level. For this reason, the loop residues were excluded from the NCS constraints, thereby allowing them to adopt different conformations in the crystallographically independent subunits. However, in all eight subunits, the loop appeared to adopt a structure virtually identical to the closed conformation observed in the DAAO·Bz complex. The only difference between the loop conformation of the $DAAO_{red}$·iTrp and DAAO·Bz models concerns the side chain of Tyr224, which, in the reduced enzyme, rotates away from the active site in order to allow iTrp binding (Figure 4). Therefore, even in the presence of a bulky ligand such as iTrp, the loop is able to shield the active site, such that both iTrp and the FAD cofactor are solvent inaccessible.

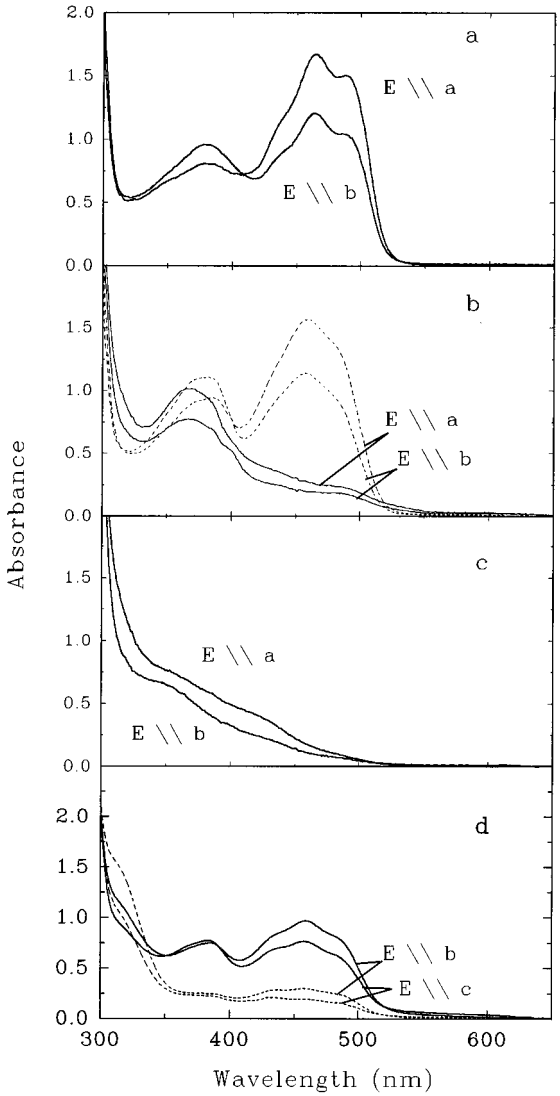

FIGURE 2: Microspectrophotometric analysis of DAAO crystals. Polarized absorption spectra were recorded on oriented crystals with the electric vector of the linearly polarized light parallel to either the *a* (E\\a), *b* (E\\b), or *c* (E\\c) crystal axis. (a) Polarized absorption spectra of a native DAAO·Bz crystal. (b) Polarized absorption spectra of a crystal soaked in 20 mM D-Arg for 48 h (solid lines) and of a crystal "back-soaked" in the standard crystal storage buffer after 48 h of soaking in D-Arg (dashed lines). (c) Polarized absorption spectra of a crystal soaked in 20 mM D-Trp. (d) Polarized absorption spectra of a crystal soaked in 20 mM kVal, recorded along the *b* and *c* crystal axes before (solid line) and after exposure to the white light beam of a 75 W Xe lamp (dashed line).

The similarity between the $DAAO_{red}$·iTrp and DAAO·Bz complexes extends also to the rest of catalytic site. The rms deviation of all atoms within 5 Å of the flavin ring is 0.43 Å. In addition to the Tyr224 rotation, the only significant movement concerns the segment Ala49−Leu51, whose backbone atoms shift away from the flavin by 0.6 Å (Figure 4). Like in the oxidized state, the flavin ring does not significantly deviate from planarity, displaying a 3° angle between the benzene and the pyrimidine rings.

[2] The possibility that, rather than the imino acid, the keto acid of Trp is bound in the active site of the reduced enzyme cannot be ruled out. This would imply that the imino acid product had dissociated from the enzyme and then hydrolyzed to the keto acid, a reaction disfavored by the high ammonium concentration (>1 M) of the crystal storage buffer (see eq 3). In any case, the conclusions drawn from the described binding studies do not depend on whether the keto acid or the imino acid is bound in the reduced enzyme catalytic center.

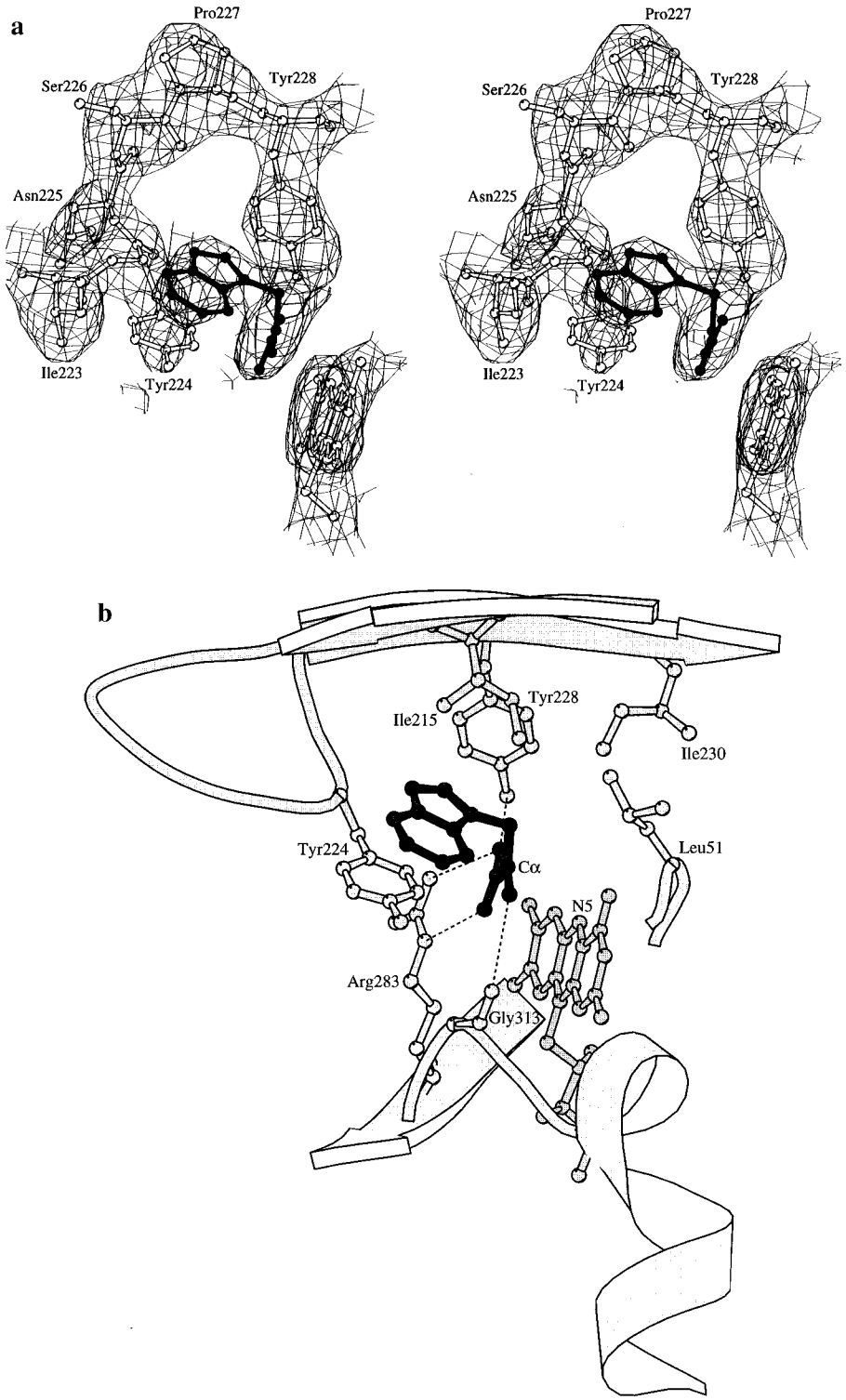

FIGURE 3: (a) Averaged omit electron density map (see Materials and Methods) for the active site residues of the $DAAO_{red}$·iTrp complex superposed to the final refined structure. The map was generated by averaging the electron density map calculated with the model resulting from rigid body refinement in which the active site residues were omitted from phase calculation. The contour level is 1σ. The flavin is in the lower right corner. It was produced with program BOBSCRIPT (R. Esnouf, personal communication), a modified version of MOLSCRIPT (Kraulis, 1991). (b) MOLSCRIPT (Kraulis, 1991) diagram of the catalytic center of the $DAAO_{red}$·iTrp complex. The protein−ligand H bonds (donor−acceptor distance of less than 3.4 Å) are represented by dashed lines.

D-Arg Soaking. DAAO is able to discriminate between positively charged amino acids, which are oxidized, and negatively charged amino acids, which are neither substrates nor inhibitors of the protein (Dixon & Kleppe, 1965). However, inspection of the substrate binding site (Figure 3b) does not reveal any feature, such as the proximity of a negatively charged residue providing electrostatic repulsion, which could explain the lack of activity toward acidic amino acids. We have tried to shed light on this problem by carrying out the structure analysis of a crystal soaked in D-Arg. Unfortunately, the resulting electron density map is not clearly interpretable. In fact, both averaged and unaveraged maps show, in proximity of the flavin, a density peak which is too small and poorly defined to be fitted by an Arg

Table 2: Refinement Statistics

DAAO complex	$DAAO_{red}$·iTrp	D-Arg soaking	$DAAO_{red}$·kVal
resolution (Å)	20−3.1	20−3.2	20−3.2
R_{factor} (%)	23.6	25.3	23.2
R_{free} (%) (1000 reflections)	25.3	28.2	26.5
number of protein atoms[a]	2642	2642	2642
rmsd from ideal values[b]			
bond lengths (Å)	0.023	0.020	0.020
bond angles (deg)	3.0	3.0	3.3
trigonal atoms (Å)	0.014	0.016	0.011
planar groups (Å)	0.016	0.017	0.016
nonbonded atoms (Å)	0.118	0.111	0.120
Δ*B* bonded atoms (Å^2)	6.2	6.7	7.1
number of water molecules	107	0	8

[a] Refinement was carried out with strict NCS constraints (eight identical subunits), except for residues 216−228, which form the active site lid. In all three structures, each protein subunit consists of residues 1−339 and a FAD molecule. As in the native structure (Mattevi et al., 1996), C-terminal residues 340−347 are disordered and not visible in the electron density maps. [b] The rms deviations from ideal values were calculated by the program TNT (Tronrud et al., 1987).

ligand. On the other hand, the microspectrophotometric analysis (Figure 2b) suggests that, upon D-Arg soaking, benzoate is displaced from the active center leading to reduction of the crystalline enzyme. On this basis and by analogy with the results of the D-Trp soaking, the electron density peak in the active site of the D-Arg-soaked crystal could be interpreted as being due to a disordered iArg molecule bound to the enzyme. Unlike iTrp, the aliphatic side chain of iArg can enjoy considerable conformational freedom such that, in the absence of specific interactions with the protein, it may well adopt multiple conformations. On the other hand, the possibility that the poor definition of the electron density peak may simply reflect a low occupancy of the iArg ligand cannot be ruled out. In any case, however, neither of these hypotheses can be supported unequivocally by the available data, preventing us from further discussing on the D-Arg soaking experiment.

Covalent Adduct with 3-Methyl-2-oxobutyric Acid (kVal). Both microspectrophotometric and crystallographic analyses revealed that soaking of kVal leads to keto acid decarboxylation and formation of a covalent bond between the keto acid Cα and flavin N5 atoms. In the refined structure, the acyl adduct is characterized by a distorted isoalloxazine moiety, which adopts a "butterfly" conformation with an angle of 22° between the benzene and the pyrimidine rings (Figure 5). The decarboxylated kVal molecule occupies the same position of iTrp in the $DAAO_{red}$·iTrp complex. Namely, the kVal aliphatic side chain is held in position by the interactions with several hydrophobic residues (Leu51, Ile230, Ile215, Tyr228, and Tyr224), whereas the kVal carbonyl oxygen makes a H bond with Arg283.

When compared to the DAAO·Bz structure, acyl adduct formation does not appear to cause any significant conformational change in the active center. Even Tyr224 and the peptide segment Ala49−Leu51, which in the iTrp complex move away from the catalytic site, adopt the same conformation observed in the benzoate structure. Furthermore, a strong electron density peak in all eight crystallographically independent subunits indicates the presence of a tightly bound water molecule (W1 in Figure 5) interacting with Tyr224, Gly313, and Gln53 and occupying the same position of the "active site water" observed in the DAAO·Bz structure (Mattevi et al., 1996).

DISCUSSION

Mechanism of Substrate Oxidation and Flavin Reduction. The catalytic mechanism of DAAO has been extensively studied by a variety of techniques (Curti et al., 1992). It was generally accepted that the reaction proceeds by abstraction of the substrate α-proton by means of a protein base, with consequent formation of a carboanion intermediate (Walsh et al., 1973; Ghisla & Massey, 1989; Curti et al., 1992). However, the DAAO·Bz structure revealed that in the catalytic center, no protein residue is properly positioned to act as the postulated active site base (Mattevi et al., 1996). On the contrary, analysis of the three-dimensional structure suggested that flavin reduction could occur via direct hydride transfer from the substrate Cα atom to the flavin N5. The $DAAO_{red}$·iTrp complex fully confirms this hypothesis (Figure 3b). The imino acid Cα atom is 3.8 Å from the flavin N5 atom. Furthermore, assuming that the binding mode of an amino acid substrate is similar to that of iTrp, the substrate α-hydrogen would be directed exactly toward the flavin ring, as required for hydride transfer. In this context, it is remarkable that the iTrp binding mode closely resembles that of the nicotinamide ring observed in several $NAD(P)^+$-dependent flavoenzymes, for which a hydride transfer mechanism has been shown to occur (Ghisla & Massey, 1989).

Comparison between the DAAO·Bz and the $DAAO_{red}$·iTrp complexes shows that there are no changes in the FAD binding site. The only noticeable difference concerns the 0.6 Å shift of Ala49−Leu51, which causes the weakening of the FAD−Ala49 H bond, with an increase of the FAD N5−N49 distance from 3.0 Å in the DAAO·Bz complex to 3.4 Å in the $DAAO_{red}$·iTrp structure (Figure 4). This movement can be rationalized by considering that, upon reduction, the flavin N5 atom most likely becomes protonated. Therefore, it can be expected that the FAD N5−Ala49 N H bond is weakened or even lost in the reduced enzyme. In this respect, it is noticeable that the Ala49−Leu51 shift occurs also in the structure resulting from the D-Arg soaking experiment, in which the flavin (Figure 2b) is reduced.

Substrate Specificity and the Role of the Active Site Lid. DAAO is characterized by a broad substrate specificity, being able to oxidize amino acids of various size and polarity, such as D-Ala, D-Trp, and D-Arg. This feature is particularly intriguing because the X-ray analysis of the DAAO·Bz complex (Mattevi et al., 1996) revealed that the active site is formed by a cavity, made solvent inaccessible by loop 216−228 (the active site lid; Figures 1 and 3b). Such an observation led to the proposal that the loop could switch during catalysis between the closed conformation of the DAAO·Bz complex and an open state, in which substrate binding and product release can take place. Such a model finds support in the limited proteolysis studies carried out by Torri Tarelli et al. (1990), which showed that the 216−228 loop is cleaved by the proteases at Arg221 in the ligand-free enzyme. On the contrary, binding of a substrate or inhibitor prevents proteolytic cleavage, in keeping with the idea that the conformation and/or flexibility of the loop is affected by the binding of an active site ligand.

Another interesting feature emerging from the analysis of the DAAO·Bz structure concerned the volume of the active

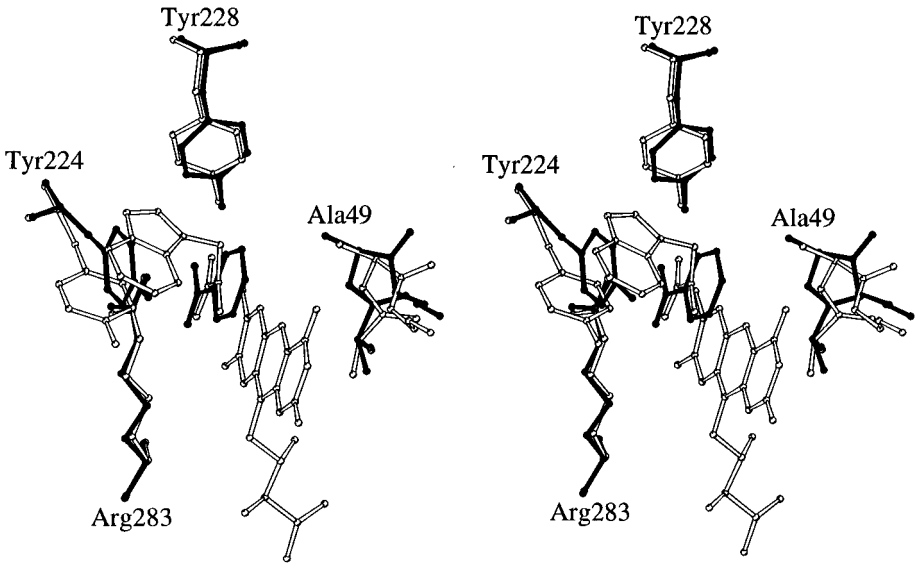

FIGURE 4: Superposition between the active center of the DAAO·Bz (closed bonds) and $DAAO_{red}$·iTrp (open bonds) complexes. For the sake of clarity, the FAD molecule of the DAAO·Bz structure is not shown.

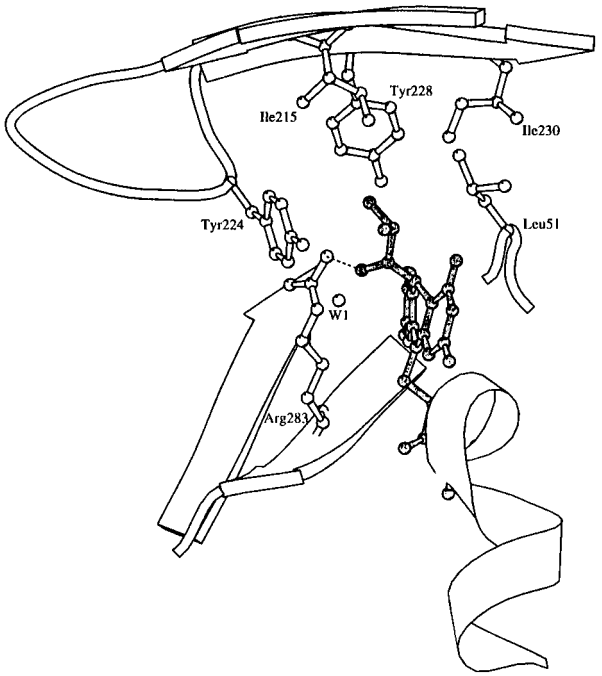

FIGURE 5: MOLSCRIPT (Kraulis, 1991) diagram of the active site of the $DAAO_{red}$·kVal complex, showing the acyl adduct−protein interactions. W1 is a water molecule which is in a well-defined electron density peak in all the eight crystallographically independent subunits.

site cavity, which is comparable to that of an amino acid bearing a four-carbon atom side chain (Mattevi et al., 1996). This fact indicated that, besides controlling the active site accessibility, the loop could play a major role also in determining the enzyme substrate specificity. To address this point, we have investigated DAAO in complex with iTrp. The structure of this complex shows that, even in the presence of the bulky iTrp ligand, the loop essentially retains the closed conformation so that the active center is solvent inaccessible. Furthermore, it turns out that room for the iTrp side chain is created through a movement of Tyr224, which rotates away with respect to the position occupied in the DAAO·Bz complex (Figure 4). Thus, Tyr224 appears to be crucial in that it adapts its conformation depending on the size of the ligand side chain. Such an adaptability is further highlighted by the $DAAO_{red}$·kVal structure, in which the small size of the ligand allows the Tyr224 aromatic ring to move into the catalytic center, adopting the same conformation observed in the DAAO·Bz complex (Figure 5).

The functionality of the active site lid as a gate opening and closing the active center may have a precise significance for the catalytic reaction mechanism. Particularly, the increased active site hydrophobicity caused by loop closure could facilitate the hydride transfer step leading to substrate oxidation. A similar phenomenon has been observed in several $NAD(P)^+$-dependent dehydrogenases [see Waldman et al. (1988) and Stoll et al. (1996) and references therein]. Also in these enzymes, shielding of the active site, through either loop closure or domain rotation, is thought to enhance the efficiency of the hydride transfer reaction leading to substrate oxidation. Thus, the presence of a structural element controlling active site accessibility seems to be a recurrent feature in those enzymes which employ a hydride transfer mechanism to carry out a redox reaction. In the case of DAAO, protein engineering studies, made possible by the recent cloning of the DAAO gene (Pollegioni et al., 1994), will provide further insight into the role of the active side lid in the enzyme catalytic cycle.

FAD Oxidation. After oxidation of the substrate, the reduced flavin is reoxidized by molecular oxygen, producing a hydrogen peroxide molecule. The crystallographic data presently available provide little information about the oxidative half-reaction. However, it is of interest to consider that flavin oxidation is thought to proceed through a 4α-hydroperoxide flavin intermediate (Massey, 1995). The latter is expected to have a distorted nonplanar conformation, due to the tetrahedral configuration of the C4α carbon atom. Indeed, the structure of the covalent adduct formed upon kVal soaking reveals that the DAAO active center is able to bind a highly distorted flavin ring (Figure 5). Thus, in addition to an adaptable substrate binding site, DAAO displays a high degree of plasticity in the flavin binding site, a feature likely to be relevant for the enzyme's function as a highly efficient oxidase.

ACKNOWLEDGMENT

It is a pleasure to thank all members of the Pavia protein crystallography group for many useful discussions. The supervision of the ELETTRA and EMBL/DESY staff during synchrotron X-ray data collection is gratefully acknowledged.

REFERENCES

Brünger, A. T. (1992) *Nature 355*, 472−475.
Collaborative Computational Project Number 4 (1994) *Acta Crystallogr. D 50*, 760−767.
Curti, B., Ronchi, S., & Simonetta, M. P. (1992) in *Chemistry and Biochemistry of Flavoenzymes* (Müller, F., Ed.) pp 69−94, CRC Press, Boca Raton, FL.
D'Aniello, A., D'Onofrio, G., Pischetola, M., D'Aniello, G., Vetere, A., Petrucelli, L., & Fisher, G. H. (1993) *J. Biol. Chem. 268*, 26941−26949.
DeKok, A., Veeger, C., & Hemmerich, P. (1974) in *Flavins and Flavoproteins* (Kamin, H., Ed.) pp 63−78, University Park Press, Baltimore.
Denu, J. M., & Fitzpatrick, P. F. (1994) *Biochemistry 33*, 4001−4007.
Dixon, M., & Kleppe, K. (1965) *Biochim. Biophys. Acta 96*, 368−382.
Fukui, K. (1996) in *Twelfth international symposium on flavins and flavoproteins*, University of Calgary, abstract I1.
Ghisla, S., & Massey, V. (1989) *Eur. J. Biochem. 181*, 1−17.
Ghisla, S., Massey, V., & Choong, Y. S. (1979) *J. Biol. Chem. 254*, 10662−10669.
Hersh, L. B., & Schuman Jorns, M. (1975) *J. Biol. Chem. 250*, 8728−8732.
Jones, T. A., Zou, J. Y., Cowan, S. W., & Kjeldgaard, M. (1991) *Acta Crystallogr. A 47*, 110−119.
Kraulis, P. J. (1991) *J. Appl. Crystallogr. 24*, 946−950.
Krebs, H. A. (1935) *Biochem. J. 29*, 1620−1625.
Laskowski, R. A., MacArthur, M. W., Moss, D. S., & Thornton, J. M. (1993) *J. Appl. Crystallogr. 26*, 283−291.
Massey, V. (1995) *J. Biol. Chem. 269*, 22459−22462.
Mattevi, A., Vanoni, M. A., Todone, F., Rizzi, M., Teplyakov, A., Coda, A., Bolognesi, M., & Curti, B. (1996) *Proc. Natl. Acad. Sci. U.S.A. 93*, 7496−7501.
Miura, R., & Miyake (1988) *Bioorg. Chem. 16*, 97−110.
Mizutani, H., Miyahara, I., Hirotsu, K., Nishima, Y., Shiga, K., Setoyama, C., & Miura, R. (1996) *J. Biochem. 120*, 14−17.
Mozzarelli, A., & Rossi, G. L. (1996) *Annu. Rev. Biophys. Biomol. Struct. 25*, 343−365.
Negri, A., Massey, V., & Williams, C. H., Jr. (1987) *J. Biol. Chem. 262*, 10026−10034.
Otwinowski, Z. (1993) in *Data collection and processing* (Sawyer, L., Isaac, N., & Bailey, S., Eds.) pp 56−62, SERC, Daresbury Laboratory, Daresbury, U.K.
Pollegioni, L., Fukui, K., & Massey, V. (1994) *J. Biol. Chem. 269*, 31666−31673.
Schell, M. J., Molliver, M. E., & Snyder, S. H. (1995) *Proc. Natl. Acad. Sci. U.S.A. 92*, 3948−3952.
Stoll, V. S., Kimber, M. S., & Pai, E. F. (1996) *Structure 4*, 437−447.
Torri Tarelli, G., Vanoni, M. A., Negri, A., & Curti, B. (1990) *J. Biol. Chem. 234*, 21242−21246.
Tronrud, D. E., Ten Eyck, L. F., & Matthews, B. W. (1987) *Acta Crystallogr. A43*, 489−501.
Waldman, A. D. B., Hart, K. W., Clarke, A. R., Wigley, D. B., Bartsow, D. A., Atkinson, T., Chia, W. N., & Holbrook, J. J. (1988) *Biochem. Biophys. Res. Commun. 150*, 752−759.
Walsh, C. T., Krodel, E., Massey, V., & Abels, R. H. (1973) *J. Biol. Chem. 248*, 1946−1951.

BI9630570